Ecological Indicators xxx (xxxx) xxx

Contents lists available at ScienceDirect

Ecological Indicators

journal homepage: www.elsevier.com/locate/ecolind

Contribution of karst ecological restoration engineering to vegetation greening in southwest China during recent decade

Yina Qiao, Yongjun Jiang *, Caiyun Zhang

Chongqing Key Laboratory of Karst Environment & School of Geographical Sciences, Southwest University, Chongqing 400715, China

ARTICLE INFO

Keywords:
Vegetation greening
Spatial-temporal variation
Climate change
Karst ecological engineering
Southwest China

ABSTRACT

General greening in vegetation, especially in southwest China, has been observed globally in recent decade. However, temporal-spatial variation patterns and potential causes of vegetation greening are not well understood in southwest China. Here, we used data of the normalized difference vegetation index (NDVI) and climate, land use and land cover, geology, ecological afforestation and karst rocky desertification to analyze the temporal-spatial variation patterns in vegetation coverage and its response to climate change and human-induced factors in southwest China between 2000 and 2016. A general greening trend in vegetation, with significant differences in temporal-spatial variation patterns, was observed in southwest China from 2000 to 2016, and the area of significant vegetation greening from 2006 to 2016 increased by 4.68% relative to the level from 2000 to 2005. The increased proportion of significant vegetation greening was higher in the karst regions (6.95%), especially in the limestone region (8.00%), than in the nonkarst region (3.82%). Of all the vegetation greening trends, 65% was associated with human-induced factors, and 35% was resulted from climate change from 2000 to 2005. After the implementation of karst ecological restoration engineering, the contribution of human-induced factors to vegetation greening increased to 77% from 2006 to 2016, although southwest China experienced a serve drought during that time. These results highlight that karst ecological engineering projects can reduce the risks of desertification and karst ecosystem sensitivity to climate perturbations.

1. Introduction

Global greening of vegetation has been observed in recent decades (Zhu et al., 2016; Keenan and Riley, 2018; Chen et al., 2019a, 2019b). Tree cover has increased by 7.1% relative to the 1982 level in global terrestrial ecosystems (Song et al., 2018). The greening of vegetation is prominent in India, China, the European Union and Canada. One of the largest global increases in vegetation biomass has occurred in southwest China, and 4% of global vegetation greening has been located in these regions over the past two decades (Brandt et al., 2018). Recent global-scale evidence has suggested a direct human impact of 60% on global vegetation greening, including grazing, deforestation and policy measures. Although urbanization, expansion of farmland and excessive deforestation have caused the vegetation degradation, soil erosion and land degradation, human land-use management has been proved to be an important driver of the global vegetation greening. (Gibbs et al., 2010; Potapov et al., 2015; Piao et al., 2015; Brandt et al., 2017; Chen et al., 2019a, 2019b). 40% of vegetation greening are associated with indirect drivers such as climate change, CO_2 fertilization effects and nitrogen deposition ((Los, 2013; Piao et al., 2015; Wang et al., 2015; Mao et al., 2016; Zhu et al., 2016; Song et al., 2018). Precipitation was considered as the main driver of the vegetation greening in arid and semi-arid regions (Fensholt et al., 2012). An increasing evapotranspiration and temperature was accompanied by a decreasing trend for vegetation greening in Asia (Lamchin et al., 2018). Additionally, extreme weather events had a great influence on the vegetation growth (Jiang et al., 2017).

Southwest China is one of the largest karst regions underlain by exposed carbonate rocks in the world. Carbonate rocks, with low amounts of soil-forming substances, are highly soluble (Yuan, 2014). Forming 1 m of soil involves dissolving 25 m thick carbonate rocks in karst regions of southwest China (Yuan and Cai, 1987; Su, 2002). Once soil is lost in karst areas, its recovery is extremely long and difficult. In addition, substantial population pressure (217 people/km^2) in southwest China karst regions results in overgrazing and over use of land and result in severe soil erosion. As a result, karst rocky desertification has

* Corresponding author at: Chongqing Key Laboratory of Karst Environment & School of Geographical Sciences of Southwest University, No. 1 Tiansheng Ave., Beibei District, Chongqing 400715, China.
E-mail address: jiangjyj@swu.edu.cn (Y. Jiang).

https://doi.org/10.1016/j.ecolind.2020.107081
Received 12 January 2020; Received in revised form 25 September 2020; Accepted 12 October 2020

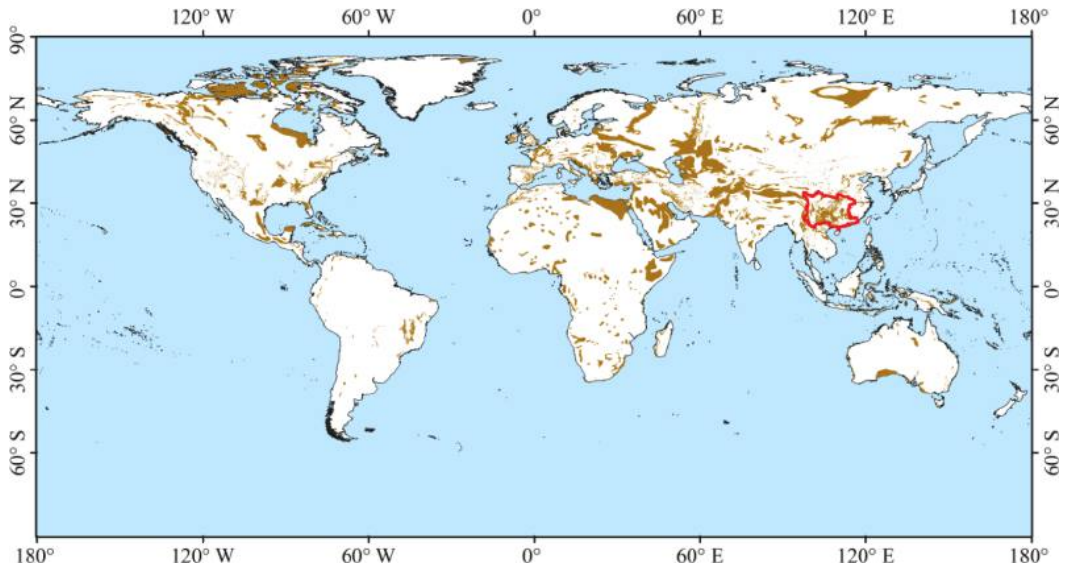

Fig. 1. Spatial patterns of global carbonate rock outcrops and location of the study area. Umber areas show regions are underlain by carbonate rocks, the white areas show regions underlain by non-carbonate rocks, and the red line delineates the study area.

reached approximately 0.13 million km^2 in 2005 (Bai et al., 2013). Land degradation is not only an environmental problem but also a social problem exacerbating the poverty level of residents who depend on agricultural products (Wang et al., 2019). To combat karst rocky desertification in southwest China, a great deal of karst ecological restoration engineering, including the Grain for Green Program, Natural Forest Protection Project and the Public welfare Forest Protection, has been carried out since 1999 in southwest China. To further combat karst rocky desertification in southwest China, "A General Plan Outline for a Program to Comprehensively Address Karst Rocky Desertification (2005–2015)" was initiated in southwest China by the central government. The karst ecological restoration engineering aim at protecting the exiting vegetation and increasing vegetation coverage to mitigate soil erosion and desertification, and further to alleviate poverty for the local residents, by closing the land for reforestation and artificial afforestation. Rural households are provided with free seedlings and compensation payments to replace sloping cropland and livestock grazing with trees and grass (Jiang et al., 2014; Tong et al., 2018). In the process of karst rocky desertification control and restoration engineering, the annual afforestation area (forest plantation, closing hill for afforestation and degraded forest restoration) increased since 2006 and increased by approximately 2.3 * 10^5 km^2 from 2006 to 2016, while the cumulative afforestation area reached nearly 3.4 * 10^6 km^2. The area of rocky desertification decreased after 2005, and the annual reduction in area

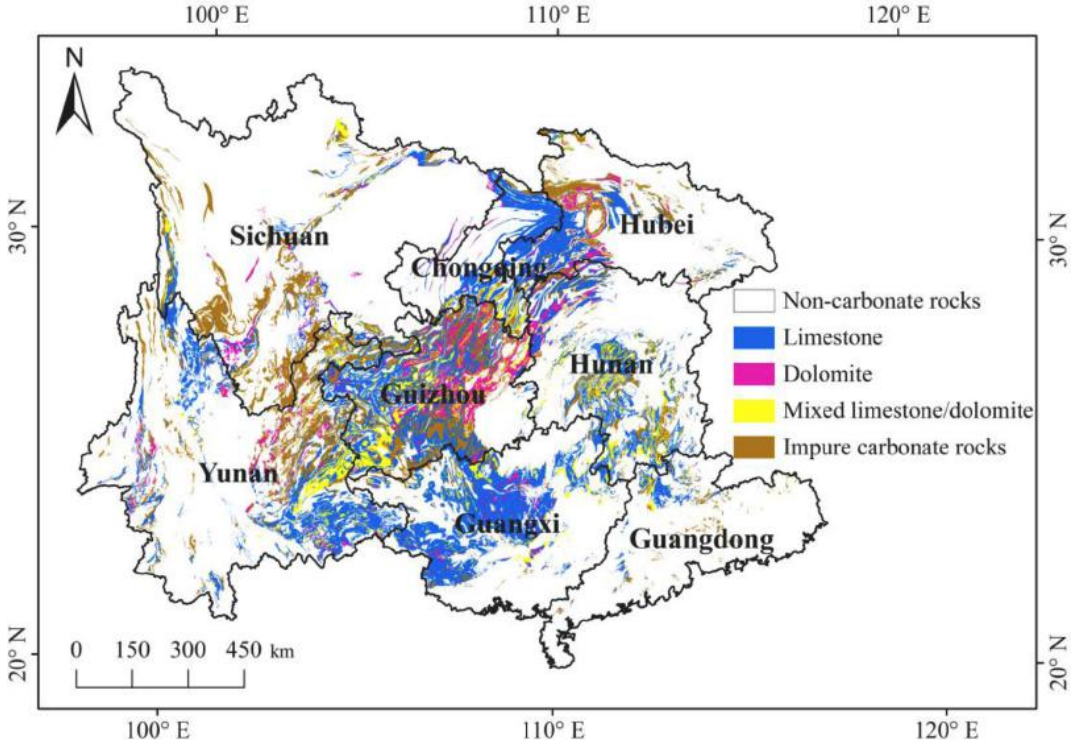

Fig. 2. Spatial patterns of carbonate rock outcrops in southwest China.

rate was 1.27% from 2005 to 2001 and 3.45% during 2005–2011.

Numerous studies have shown the vegetation greening trend in the southwest China over the past two decades (Cai et al., 2014; Wang et al., 2015; Tong et al., 2016), and indicated that vegetation greening in southwest China was attributed to the afforestation and conservation of natural forests. The great changes in land use types resulting from ecological restoration projects in recent decades were considered to be the driver for vegetation greening in southwest China (Tong et al., 2018; Brandt et al., 2018). In addition, a number of studies have investigated the impacts of climate on vegetation greening in southwest China. Temperature has been considered a limiting factor for vegetation greening due to abundant precipitation in southwest China (Hou et al., 2015). However, a few studies have shown vegetation growth in karst regions was susceptible to water stress (Lian et al., 2015; Wan et al., 2016; Zhou et al., 2018). Meanwhile, several studies have indicated that carbonate and non-carbonate rocks have significant differences in landscape morphology, soil development and water availability, and the characteristics of different carbonate rocks, mainly dolomite and limestone, impose different environmental constraints on vegetation growth (Pei et al., 2019; Qiao et al., 2020). Field surveys have revealed that the differences between dolomite and limestone determine the ways of rocks dissolution, and result in the different ways of using rainfall by vegetation (Wang et al., 2004b; Peng et al., 2019a, 2019b). However, the response of vegetation greening to climate change in different lithology regions in karst area have not been studied yet. A large number of studies investigated effects of climate and ecological restoration engineering on vegetation greening in southwest China, it remains unclear of the relative importance of the two drivers. To date, few studies focused on quantitatively identifying the contributions of climate change and human-induced factors to vegetation greening in southwest China. To evaluate the contribution of ecological restoration engineering, a prerequisite is to distinguish between climate change and human-induced greening trend in vegetation.

Remote sensing data have great potential to monitor ecological environment. Normalized Difference Vegetation Index (NDVI), based on the red and near-infrared spectrum, has been widely used to monitor vegetation activities at regional and global scales. The present study used NDVI time-series data to detect the vegetation greening, and combined of the time-series of NDVI and climate data to identify the climate-driven and human-driven vegetation greening. The Comprehensive information of the effectiveness of karst ecological restoration engineering is necessary for sustainable ecosystem management in southwest China. Therefore, the objectives of this study are (1) to assess the temporal-spatial variation patterns in vegetation greening, and (2) to quantitatively distinguish the contributions of karst ecological restoration engineering on vegetation greening in southwest China.

2. Materials and methods

2.1. Study area

The study area (20°13′-34°19′N and 97°21′-117°19′E) is located in southwest China, covering the entire karst regions in southwest China, and includes Yunnan, Guizhou, Sichuan, Chongqing, Guangxi, Guangdong, Hunan and Hubei provinces (19.5×10^5 km^2) (Fig. 1). Twenty-eight percent of the study area (5.4×10^5 km^2) is karst, which is underlain by exposed carbonate rocks. Carbonate rocks consist of limestone (50.07%), dolomite (8.75%), mixed limestone/dolomite (10.13%) and impure carbonate rocks (31.05%) (Fig. 2). The rocky desertification reached 24% of the exposed carbonate rocks areas in southwest China in 2005 (Fig. 3).

2.2. Data and processing

The normalized difference vegetation index (NDVI) was utilized to detect vegetation coverage change. The NDVI dataset used in this study was MODIS NDVI with a spatial resolution of 250 m and a temporal resolution of 16 days from 2000 to 2016. The annual maximum NDVI time series were obtained from the monthly NDVI by the maximum value composite (MVC) method to represent the best vegetation growth status in a single year (Peng et al., 2019a, 2019b). The land use type dataset was MODIS MCD12Q1 land use/cover at a 500 m spatial

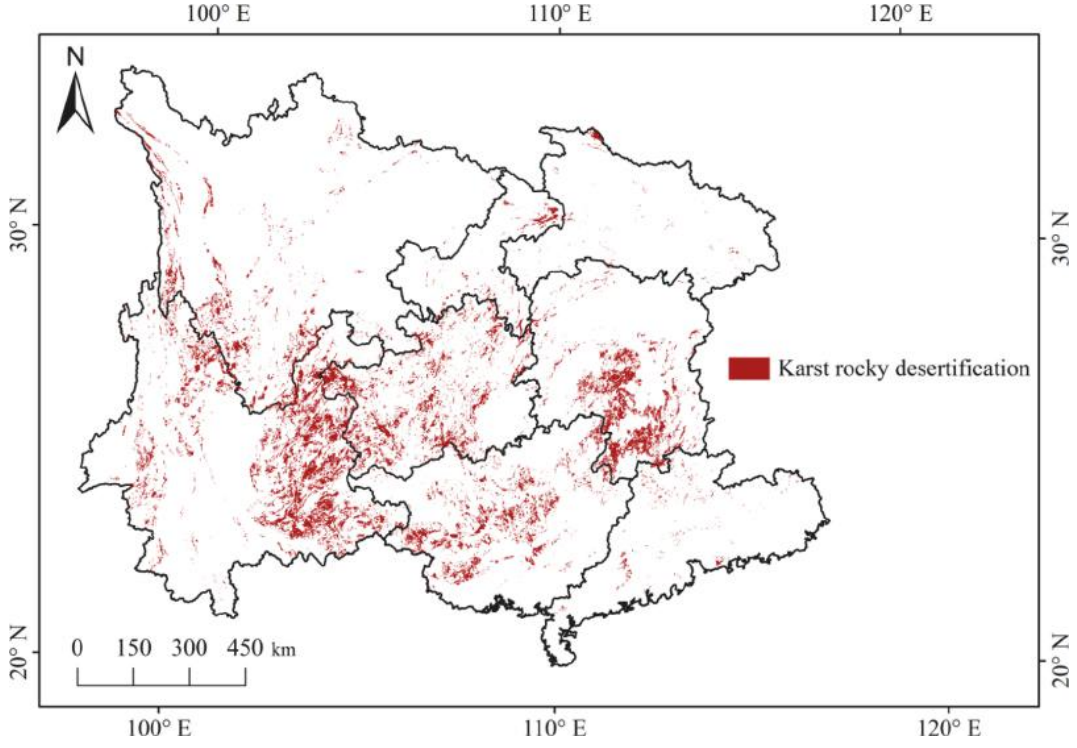

Fig. 3. Distribution of karst rocky desertification area in southwest China in 2005.

resolution. The MODIS data were derived from the LAADS DAAC (https://ladsweb.modaps.eosdis.nasa.gov/).

Temperature and precipitation data for 245 meteorological stations in southwest China from 2000 to 2016 were collected from the Chinese Meteorological Information Center (http://data.cma.cn/). The spatial patterns of annual average temperature and annual precipitation were predicted using thin-plate smoothing splines interpolation in ANUSPLIN 4.4 (Hutchinson and Xu, 2013) from the climate data.

The spatial patterns of carbonate rocks in southwest China were collected from the Institute of Karst Geology, Chinese Academy of Geological Sciences (http://en.cags.ac.cn/).

The afforestation area data were derived from the National Bureau of Statistics of China (http://www.stats.gov.cn/).

The karst rocky desertification area data were collected from State Forestry Administration of China (http://www.forestry.gov.cn/portal/zsxh/s/3445/content-548741.html).

2.3. Methods

2.3.1. Linear regression analysis

The temporal-spatial variation of the NDVI, temperature and precipitation were calculated by a linear regression.

formula is:

$$\beta = \frac{n \times \sum_{i=1}^{n} i \times A_i - \sum_{i=1}^{n} i \sum_{i=1}^{n} A_i}{n \times \sum_{i=1}^{n} i^2 - \left(\sum_{i=1}^{n} A_i\right)^2} \quad (1)$$

where n is the number of years andA_i is the variable value in year i. β indicates the direction and magnitude of the temporal variation: positive slope ($\beta > 0$) exhibits an uptrend of the variables, and negative slope ($\beta < 0$) denotes a downtrend of the variables.

The significance of the NDVI trend was examined by F test at a confidence level of 95%, NDVI trends were categorized as four levels: significant increase ($\beta_{NDVI} > 0$, $p \leq 0.05$), nonsignificant increase ($\beta_{NDVI} > 0$, $p > 0.05$) significant decrease ($\beta_{NDVI} \leq 0$, $p \leq 0.05$) and nonsignificant decrease ($\beta_{NDVI} \leq 0$, $p > 0.05$). For evaluating the vegetation coverage changes, the trends were divided into two types: vegetation greening ($\beta_{NDVI} > 0$) and vegetation browning ($\beta_{NDVI} \leq 0$).

2.3.2. Mann-Kendall test

The Mann-Kendall test, a non-parametric test method that does not assume any distributional form for the data, is widely used to identify the change point in the considered time series data (Mohsin and Gough, 2009; Tong et al., 2017; Chen et al., 2019a, 2019b). The Mann-Kendall test was adopted to detect the turning year of the vegetation coverage change. The test statistic is defined as follows:

For $NDVI_i$ time series,

$$dk = \sum_{i=1}^{k} NDVIi \quad (2)$$

$$Var(dk) = \frac{k(k-1)(2k+5)}{72} \quad (3)$$

$$E(dk) = \frac{k(k-1)}{4} \quad (4)$$

$$UFk = \frac{dk - E(dk)}{\sqrt{\mathrm{var}(dk)}} \quad (5)$$

where $NDVI_i$ represents the NDVI value for the year i, and k represents the length of the time series. The UB_k is the backward statistical sequence generated with the reverse data series of $NDVI_i$, it was calculated by the formula (2)–(5).

When the UF values are more than zero, it indicates an uptrend in NDVI, otherwise the values indicate a downtrend in NDVI. UB curve is used to search for an abrupt change in the NDVI trend. The intersection point of the two sequence curves within the confidence interval ($p < 0.05$, the interval is ± 1.96) indicates the change year of NDVI trend. Assuming that long-term change in vegetation coverage was only affected by climate change and human-induced factors, and thus this turning point was caused by the climate change and human-induced factors. In order to analyze the drivers for this significant change in vegetation coverage trend, based on the year corresponding to the turning point, the time series (2000–2016) was divided into two periods.

2.3.3. Correlation analysis

The Pearson correlation coefficients (R) between the NDVI and climate variables were calculated in each pixel to indicate the impact of climate on vegetation greening. Correlations with $p \leq 0.05$ are considered to be significant. Therefore, the correlations between vegetation greening and climate variables were classified to four types: significantly positive correlation ($R > 0$, $p \leq 0.05$), nonsignificantly positive correlation ($R > 0$, $p > 0.05$), significantly negative correlation ($R < 0$, $p \leq 0.05$), and nonsignificantly negative correlation ($R < 0$, $p > 0.05$). The spatial patterns of the contribution of human-induced factors to vegetation coverage change and driving factors of vegetation greening were calculated respectively in two periods based on the turning point to reveal the effects of karst ecological restoration engineering.

2.3.4. Residual analysis

The residual analysis has been widely used to distinguish the contributions of climate change and human-induced factors to vegetation greening (Huber et al., 2011; Wessels et al., 2012; Tong et al., 2016; Duo et al., 2016). We assumed that NDVI was only affected by climate change and human activities. The residual analysis is based on the observation that a strong relationship exists between NDVI and climate (temperature and precipitation). If the influences of climate are removed from the NDVI time series, then the residuals can be attributed to the effects of human-induced factors. The method has three steps. First, A pixel-based multiple linear regression between the annual NDVI ($NDVI$) and annual temperature (T) and precipitation (P) was established, and the regression coefficients ($a, b_1,$ and b_2) were used to predict the annual NDVI ($NDVI_{pre}$) in each pixel.

$$NDVI_{pre} = a + b_1 T + b_2 P \quad (6)$$

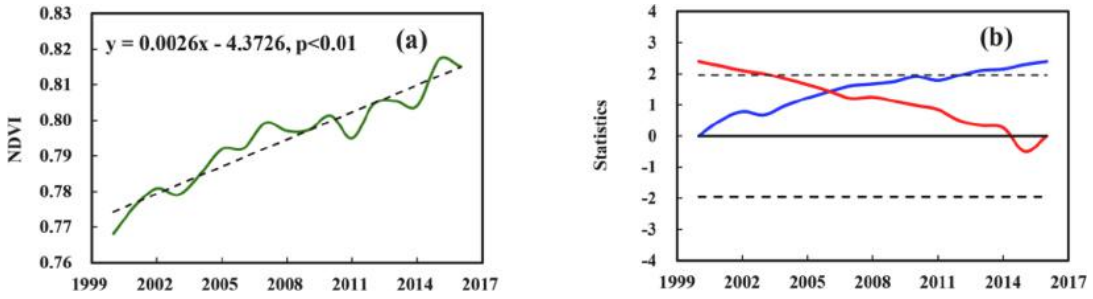

Fig. 4. Interannual change (a) and turning point (b) in the NDVI (2000–2016).

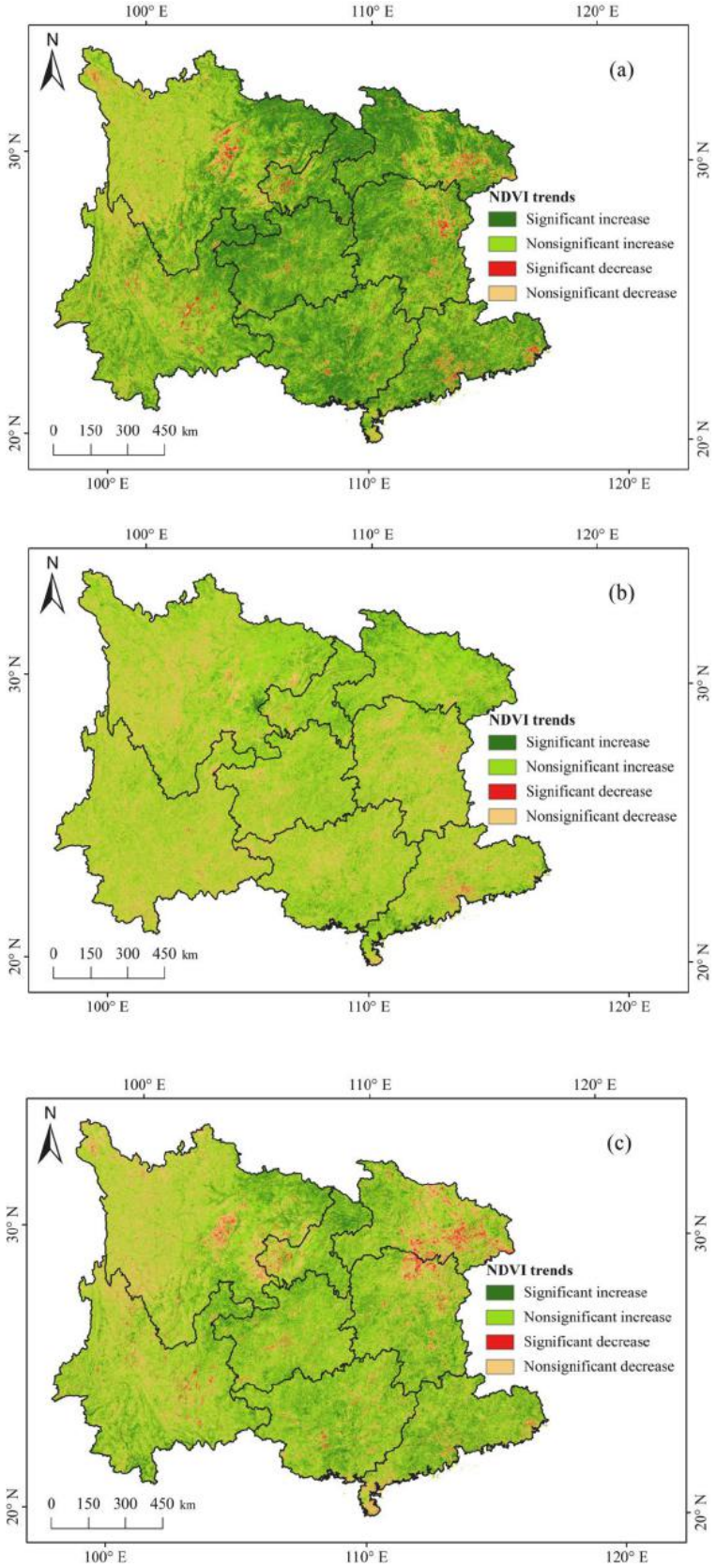

Fig. 5. Spatial patterns of the NDVI trends in different periods (2000–2016 (a), 2000–2005 (b) and 2006–2016 (c)).

Table 1
Annual rate of the NDVI change and the proportion of significant NDVI trends in 2000–2005 and 2006–2016 for the different regions.

Regions	Time period	Rate	Significant increase	Significant decrease
Southwest China	2000–2005	0.0041	7.39%	1.38%
	2006–2016	0.0021	12.07%	2.63%
Nonkarst	2000–2005	0.0041	7.46%	1.43%
	2006–2016	0.0018	11.28%	2.82%
Karst	2000–2005	0.0041	7.22%	1.26%
	2006–2016	0.0029	14.17%	1.57%
Limestone	2000–2005	0.0040	7.20%	1.28%
	2006–2016	0.0031	15.20%	1.41%
Dolomite	2000–2005	0.0048	8.36%	1.01%
	2006–2016	0.0027	12.77%	1.99%
Mixed limestone/ dolomite	2000–2005	0.0038	6.56%	1.41%
	2006–2016	0.0029	13.79%	2.01%
Impure carbonate rocks	2000–2005	0.0040	7.15%	1.24%
	2006–2016	0.0026	13.04%	1.55%

Then, the residuals were calculated for each pixel between the observed annual NDVI and predicted annual NDVI, which represented the remaining observed NDVI value that were not explained by precipitation and temperature.

$$NDVI_{res} = NDVI - NDVI_{pre} \quad (7)$$

The changes in the $NDVI_{pre}$ ($\beta_{NDVI_{pre}}$) and $NDVI_{res}$ ($\beta_{NDVI_{res}}$) were calculated based on Eq. (1). Finally, the contribution of human-induced factors (C_{human}) and climate change ($C_{climate}$) to the vegetation coverage change were defined (Pan et al., 2017; Qi et al., 2019):

$$C_{human} = \frac{\beta_{NDVI_{res}}}{\beta_{NDVI}} \times 100\% \quad (8)$$

$$C_{climate} = \frac{\beta_{NDVI_{pre}}}{\beta_{NDVI}} \times 100\% \quad (9)$$

A negative C_{human} value indicates the contribution rate of climate change to vegetation coverage change is 100% ($C_{human} = 0$, $C_{climate} = 100\%$), and a negative $C_{climate}$ value means the contribution rate of human-induced factors to vegetation coverage change is 100% ($C_{human} = 100\%$, $C_{climate} = 0$). When $\beta_{NDVI} > 0$ and $C_{human} > 50\%$, human-induced factors dominate the vegetation greening; $\beta_{NDVI} > 0$ and $C_{climate} > 50\%$ suggests climate change dominate the vegetation greening. The spatial patterns of the contribution of human-induced factors to vegetation coverage change and driving factors of vegetation greening were calculated in two periods based on the turning point to reveal the effects of karst ecological restoration engineering.

3. Results

3.1. Temporal-spatial variation patterns in vegetation coverage

3.1.1. Temporal variation patterns in vegetation coverage

At the regional scale, the NDVI showed a significantly increasing trend at the rate of 0.0026 year^{-1} from 2000 to 2016 ($p < 0.01$) (Fig. 4a). As shown in Fig. 4b, the positive values of the forward sequence (UF) exceeded the confidence interval ($p < 0.05$) after 2011, and the curves of UF and UB intersected in around 2006, indicating there was a significant change in the increasing trend of NDVI. In order to compare the differences in vegetation greening before and after the turning year, and identify the drivers for this significant change in vegetation greening, based on the turning year, the time period was divided into 2000–2005 and 2006–2016.

At the pixel scale, >77% of southwest China showed an increasing trend in the NDVI, and 23% showed a decreasing trend from 2000 to 2016. The differences in the NDVI change between the two time periods were represented by the NDVI trends, namely, the area with a significant NDVI change ($p < 0.05$), were more accurate than that by the rate of NDVI change due to different time lengths in the two-time series. A significant change in the NDVI was detected in 23% of the study area between the two periods, of which 61% showed a trend from a nonsignificant to significant increasing trend (Fig. 5). The area of significant increasing and decreasing trends in the NDVI increased by 153,438 km^2 and 24,979 km^2 after 2005, respectively, during the observed 17 years. Overall, vegetation showed a greening trend from 2000 to 2016, and the greening trend was more significant from 2006 to 2016 than from 2000 to 2005 in southwest China.

3.1.2. Spatial variation patterns in vegetation coverage

As shown in Table 1, notable differences in the NDVI change were found in different regions between the two periods. The same average annual NDVI increase rate (0.0041 year^{-1}) was detected in nonkarst and karst regions from 2000 to 2005. During 2006–2016, the increasing rate of the NDVI in the karst regions (0.0029 year^{-1}), especially in the limestone area (0.0031 year^{-1}), was higher than that in the nonkarst region (0.0018 year^{-1}). At the pixel scale, the same phenomenon as at the regional scale was observed in each region (Fig. 5). The largest increase in the proportion of the significantly increasing trend in the NDVI was observed in the karst regions (6.95%), especially in the limestone area (8.00%).

3.2. Spatiotemporal change in climate

A weak warming trend was observed in southwest China from 2000 to 2016, and the annual average temperature increased to a maximum value in 2006 and fluctuated greatly during 2006–2016 (Fig. 6a). The annual mean precipitation showed a decreasing trend during the

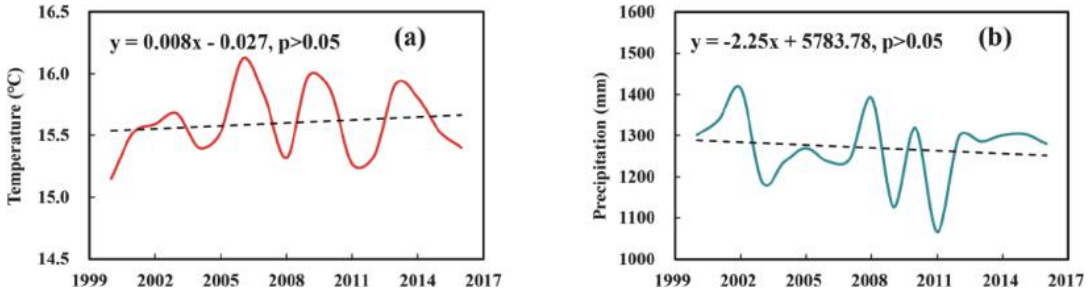

Fig. 6. Interannual changes in annual average temperature and precipitation (2000–2016).

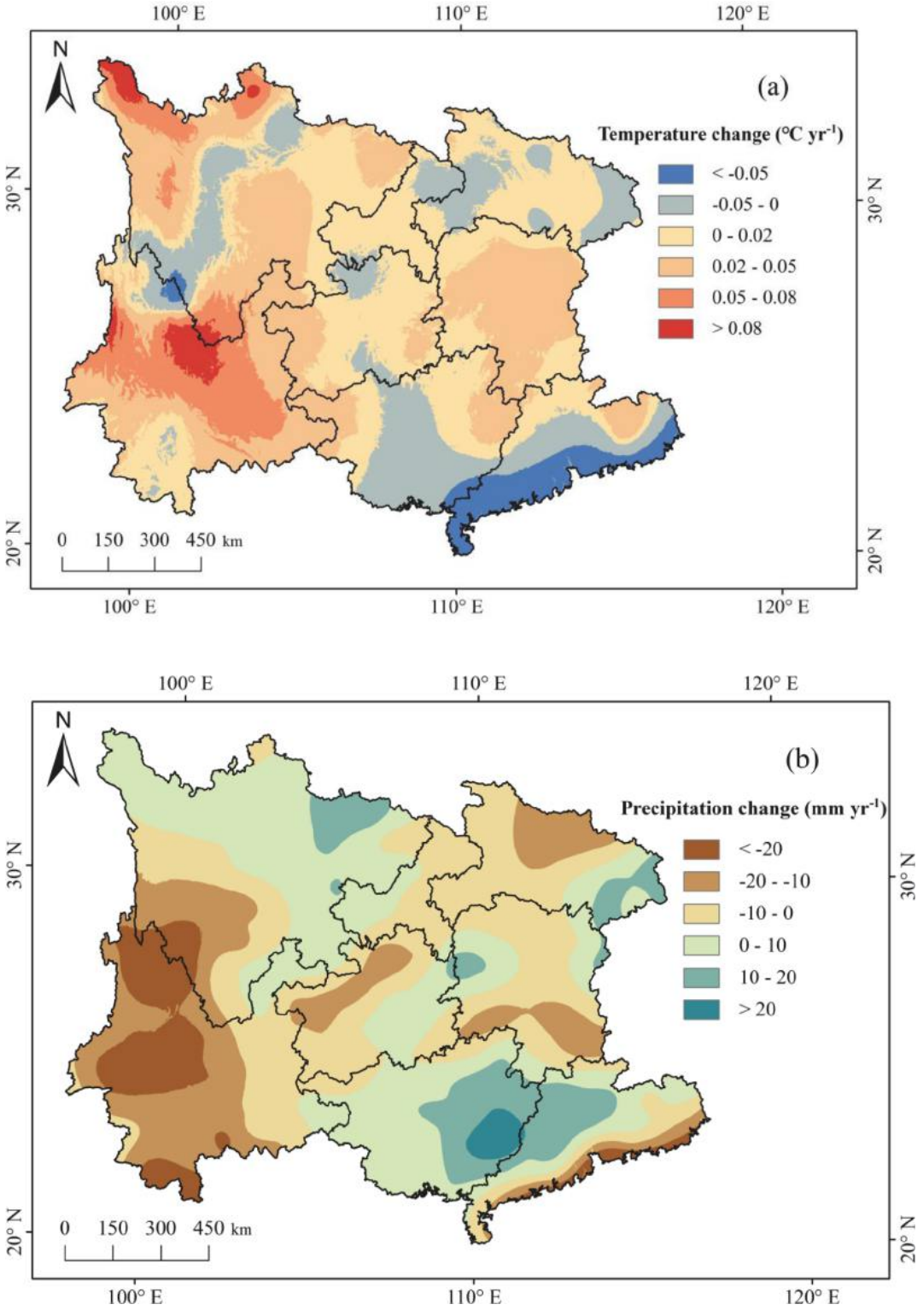

Fig. 7. Spatial patterns of the annual changes in the annual average temperature (a) and precipitation (b) from 2000 to 2016.

observed 17 years, decreased to minimum values in years approximately 2010 and became increasingly favorable from 2011 to 2016 (Fig. 6b).

Spatially, 76% of the study area showed a positive temperature slope, while 58% of the area showed a negative precipitation slope during the observed 17 years (Fig. 7). Approximately 70% of the karst regions showed warming and drying climates during 2000–2016.

According to the turning point in the NDVI change, the climate change was divided into two periods (2000–2005 and 2006–2016). There was no significant difference in temperature and precipitation between the two time periods ($p > 0.05$). The average temperature from 2000 to 2005 was lower than that from 2006 to 2016, and the average annual precipitation in 2006–2016 was 32 mm less than that in 2000–2005. In addition, climate trends were relatively unstable after 2005 (Fig. 6), therefore, southwest China had a relatively moderate climate from 2000 to 2005 and a relatively dry climate during 2006–2016. The results are consistent with previous studies in

Table 2
Transition matrix of land use types between 2000 and 2005 and between 2006 and 2016 (km^2).

	2005					
2000	Forestland	Grassland	Cropland	Water	Urban land	Barren land
Forestland	300,290	31,817	21	13	6	1
Grassland	28,954	1,222,645	46,608	714	1,289	555
Cropland	9	19,376	247,099	29	885	2
Water	19	1355	13	15,259	180	142
Urban land	0	0	0	0	26,788	0
Barren land	1	772	0	120	145	7210
	2016					
2006	Forestland	Grassland	Cropland	Water	Urban land	Barren land
Forestland	300,910	28,319	17	24	2	0
Grassland	100,710	1,128,423	40,589	3497	2193	554
Cropland	201	50,024	242,624	206	679	8
Water	20	772	25	15,156	55	106
Urban land	0	0	0	0	29,292	0
Barren land	3	1294	0	251	31	6332

southwest China, which argued the regions experienced extreme drought in 2006 and around 2010 (Li et al., 2011; Yuan et al., 2015).

3.3. Conversion of land use types from 2000 to 2016

Grassland and barren land areas continuously decreased, with net losses in area of 91,932 and 1250 km^2, respectively, while urban land areas continuously increased, with a net increase in area of 2960 km^2 between 2000 and 2016 (Table 2).

During 2000–2005, 60% of the loss of grassland area was converted to croplands (46,608 km^2). The increase in cropland accounted for the primary increase in land use in karst regions (46%). Forestlands decreased by 2875 km^2, and croplands increased by 26,341 km^2 (Table 2). The expansion of urban lands mainly encroached upon grasslands and croplands (2174 km^2).

During 2006–2016, 98% of the loss in croplands was due to conversion to grasslands and forestlands (50,225 km^2). Increases in forestland accounted for the main increase in land use in karst regions (45%). Forestlands increased by 72,571 km^2, and croplands decreased by 10,485 km^2. The expansion of urban lands encroached upon substantial natural land resources (2872 km^2).

4. Discussion

4.1. Contribution of climate change and human-induced factors to vegetation greening

Vegetation cover change is commonly considered to be triggered by climatic factors and human-induced factors, separately or together, to influence vegetation greening at regional and global scales (King et al., 2015; Qi et al., 2019). Thus, quantitatively identifying the contributions of climate and human-induced factors to vegetation greening is critical for developing adaptation strategies. As shown in Fig. 8, the contribution rate of human-induced factors to NDVI change increased from 60% in 2000–2005 to 70% in 2006–2016. Sixty-five percent of the vegetation greening was mainly associated with human-induced factors, while climate change influenced 35% of the vegetation greening from 2000 to 2005 in southwest China. The proportion of vegetation greening driven by human-induced factors increased to 77% throughout southwest China and was as high as 81% in karst regions from 2006 to 2016 (Fig. 8).

4.2. Climate-driven greening trend in vegetation—difference between the karst and nonkarst regions

4.2.1. Impact of temperature on vegetation greening—difference between the karst and nonkarst regions

Temperature had a general positive correlation with vegetation growth ($R = 0.053$), and the correlation showed no significant difference between the karst and nonkarst regions under a moderate climate (2000–2005). Increasing temperature will promote photosynthesis, which is conducive to vegetation growth. Although increasing temperature has a positive effect on vegetation growth, it also affects water availability. Rising temperatures accelerate surface water evaporation in a dry period, which limits vegetation growth. Therefore, an overall negative correlation coefficient was detected between the NDVI and temperature from 2006 to 2016, and remarkable differences in the correlations were apparent in the different regions (Table 3). Specifically, most karst regions showed correlations between the NDVI and temperature change ranging from positive to negative (Fig. 9), and temperature had more negative effects on vegetation growth in the karst regions ($R = -0.041$) than in the nonkarst region ($R = -0.014$). A karst ecosystem is characterized by a thin soil layer and weak water storage capacity; consequently, vegetation growth is more likely to be suppressed by increasing temperature (Cai, 1989; Wang et al., 2004a; Yuan, 2014). Irrigation may mitigate intense evaporation under drought conditions; therefore, a weak negative correlation between the NDVI and temperature was detected in the mixed limestone and dolomite region with more farmlands.

4.2.2. Impact of precipitation on vegetation greening—difference between the karst and nonkarst regions

Precipitation promoted vegetation growth from 2000 to 2016 in southwest China. The correlation relationships between the NDVI and precipitation were stronger in the relatively dry period (2006–2016) than under relatively moderate climate (2000–2005). The differences in the correlations among the regions are highlighted in Table 3. The correlation coefficient between the NDVI and precipitation was significantly higher in the nonkarst region than in the karst regions from 2000 to 2005, which indicates that the responses of vegetation in the nonkarst region to precipitation are more prominent under a moderate climate. Developed underground hydrological structures with numerous fissures and conduits allow rainfall to quickly percolate into the underground river network (Zhou et al., 2018). As a result, direct utilization of rainfall by vegetation is lower in karst regions, rendering the correlations between the NDVI and precipitation weak in the karst regions. However, stronger positive correlations between the NDVI and precipitation were found in most karst regions (Fig. 9), and there were higher correlation coefficients for the karst regions in the dry periods (2006–2016) (Table 3). The main reason for this difference may be attributed to the shortage of underground water due to drought and weak soil water storage capacities in the karst regions. Additionally, sparse vegetation cover induced by karst rocky desertification in some places may result in rapid evaporation of soil water during the drought. Thus, the water requirement for vegetation growth heavily depended on precipitation in karst regions from 2006 to 2016.

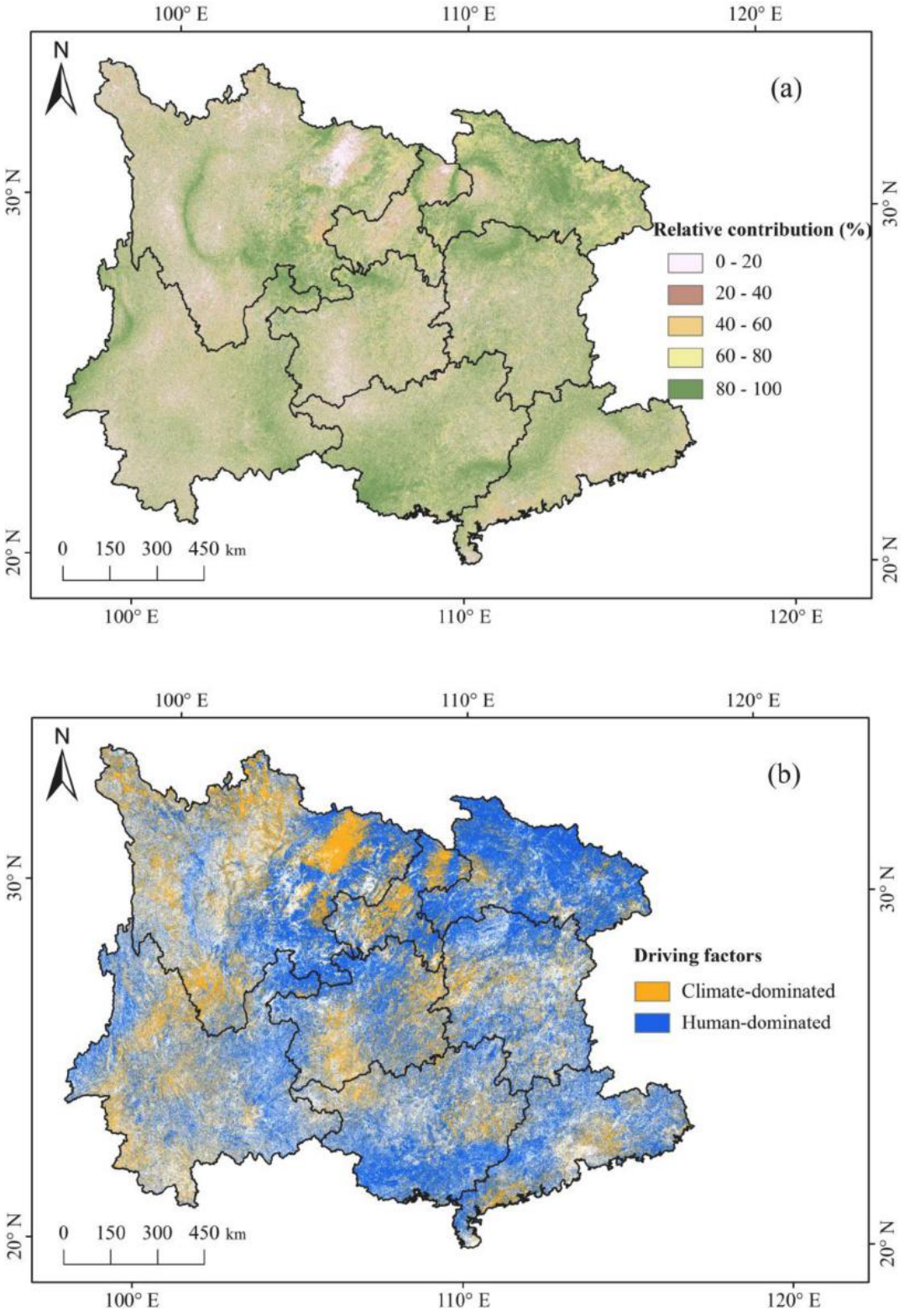

Fig. 8. Spatial patterns of the contribution of human-induced factors to vegetation coverage change and driving factors of vegetation greening in 2000–2005 (a and b) and 2006–2016 (c and d).

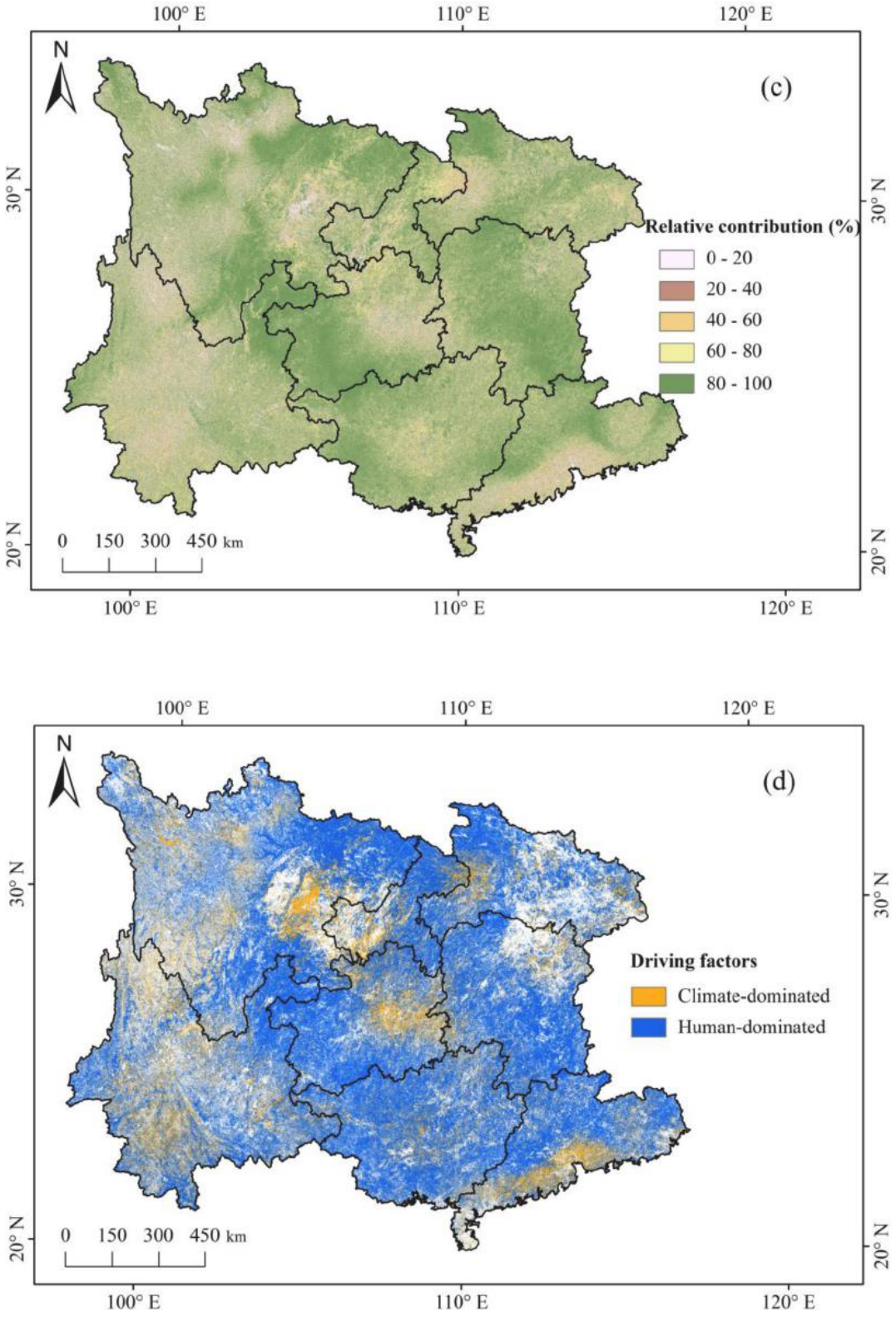

Fig. 8. (*continued*).

In summary, vegetation growth is generally more sensitive to drought in the karst regions than in the nonkarst region. Temperature is the main climate factor affecting vegetation greening under a moderate climate, while precipitation is the important climate factor affecting vegetation greening under drought in southwest China, especially in the karst regions. However, <6% of the area showed a significant relationship between the NDVI and climate, indicating that climate change is not the main driver of vegetation greening.

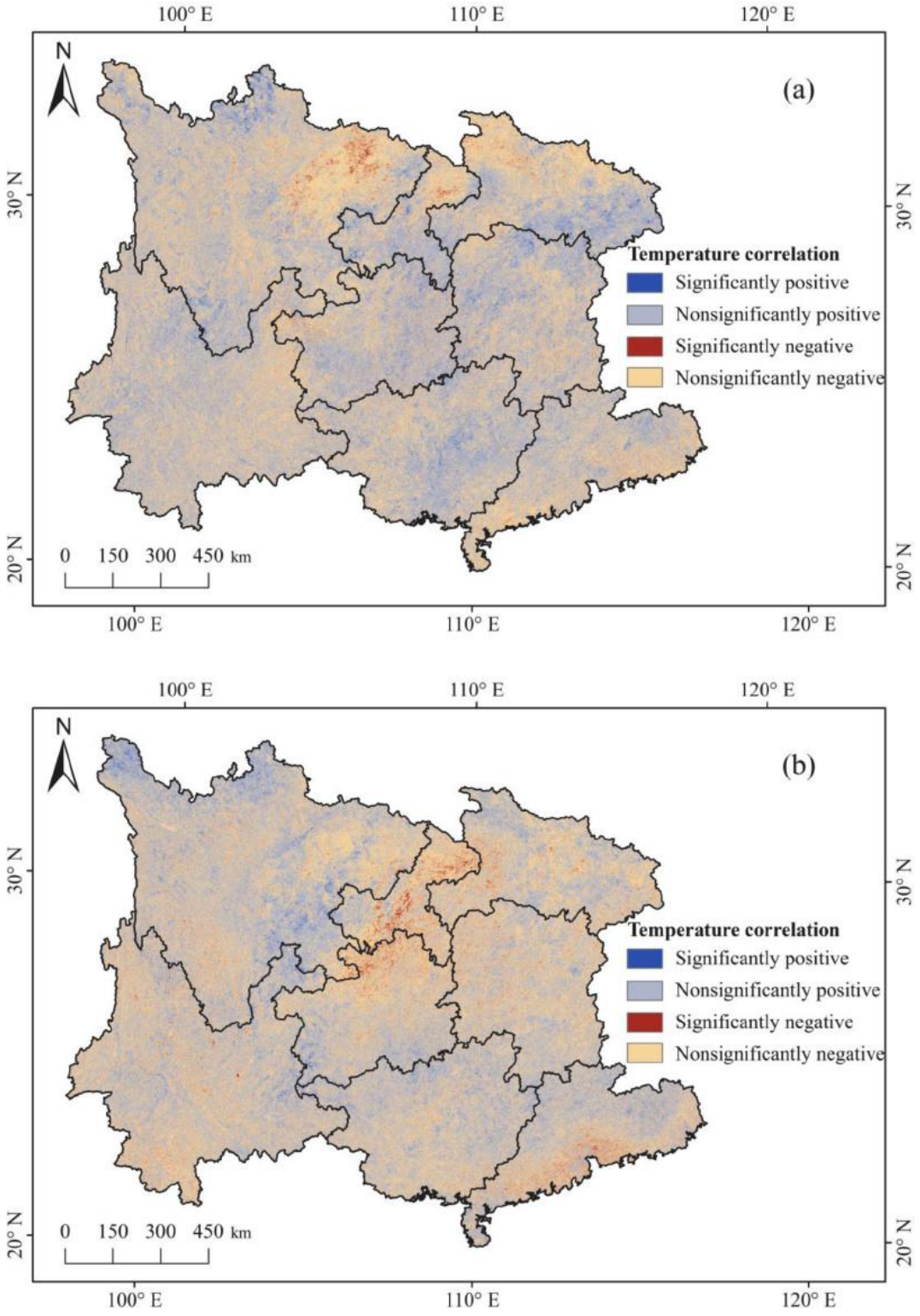

Fig. 9. Spatial patterns of the correlation coefficients between vegetation and temperature (2000–2005 (a) and 2006–2016 (b)) and precipitation (2000–2005 (c) and 2006–2016 (d)).

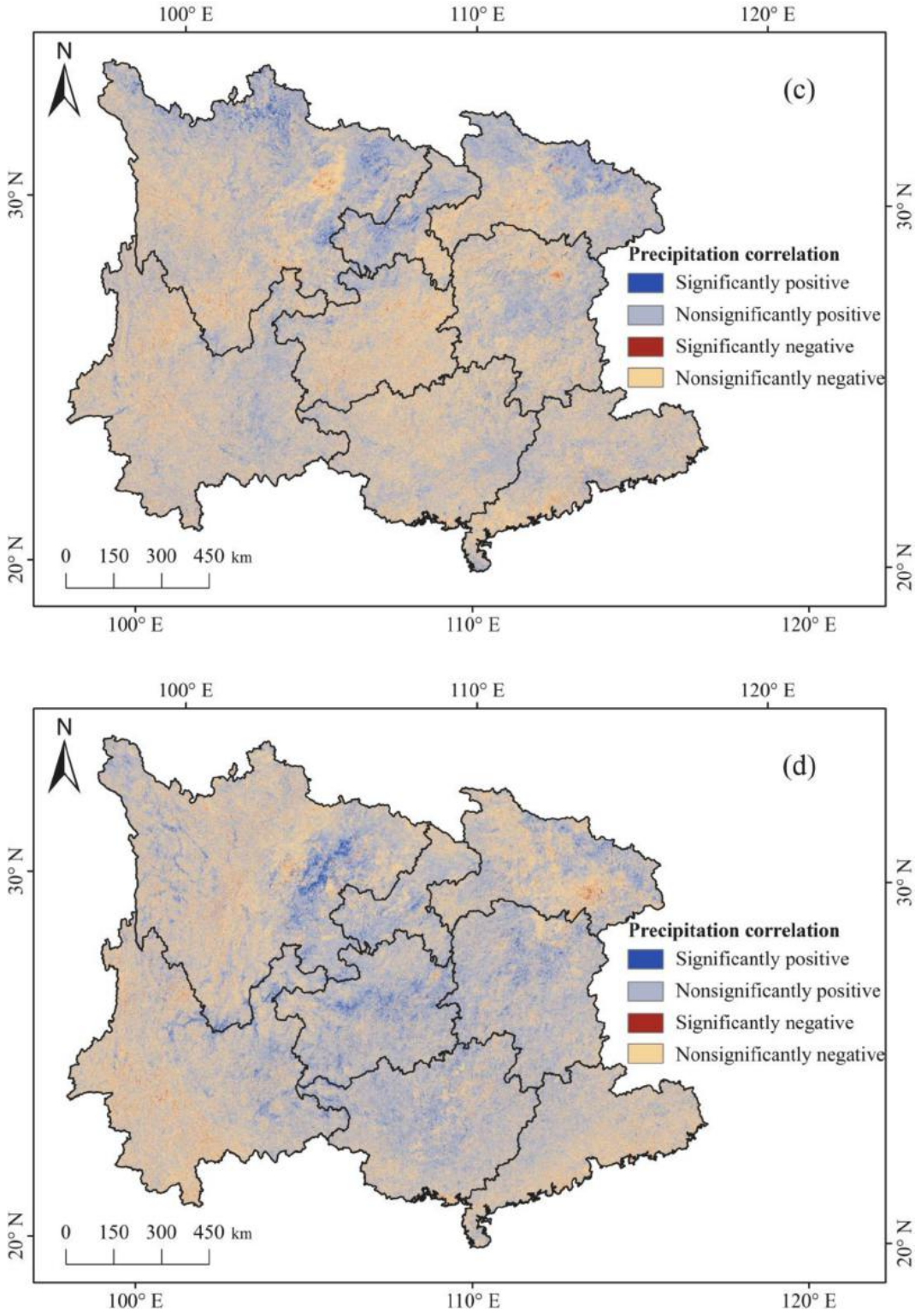

Fig. 9. (*continued*).

4.3. Karst ecological restoration engineering drives vegetation greening in southwest China

Our results indicate that human-induced factors have a remarkable impact on vegetation greening in southwest China during the past two decades, which is consistent with the results of previous studies (Tong et al., 2018; Zhang et al., 2018). Since the launch of afforestation efforts in 1999, general vegetation greening was observed throughout southwest China. The timing of the turning point in the NDVI increase was consistent with the planning of karst rocky desertification comprehensive control and restoration projects. Vegetation recovery in the karst regions was mostly pronounced, and the proportion of karst vegetation greening driven by human-induced factors increased to 81% after conservation. Therefore, it can be assumed that karst ecological restoration

Table 3
Pearson correlations between the NDVI and climate factors for different regions in 2000–2005 and 2006–2016.

Regions	Temperature		Precipitation	
	2000–2005	2006–2016	2000–2005	2006–2016
Southwest China	0.055	−0.022	0.037	0.075
Nonkarst	0.053	−0.014	0.047	0.061
Karst	0.058	−0.041	0.012	0.112
Limestone	0.060	−0.047	0.007	0.114
Dolomite	0.085	−0.085	0.004	0.116
Mixed limestone/ dolomite	0.062	−0.006	0.009	0.147
Impure carbonate rocks	0.048	−0.031	0.023	0.094

projects are considered human-induced factors in terms of karst vegetation greening. There was a noticeable net decrease in farmland area (10,485 km^2), which mostly returned to grassland, and a remarkable increase in forestland area (72,571 km^2) from 2006 to 2016 in contrast to the expansion of croplands during 2000–2005 in southwest China. This natural vegetation restoration was consistent with the aim of ecological restoration projects, indicating that land use changes in recent decades largely occur due to karst ecological conservation projects.

The increase in afforestation area since 2006 was considerable (Fig. 10a), and a strong correlation between the NDVI and the cumulative afforestation area was observed from 2000 to 2016 ($R^2 = 0.9$, $p < 0.01$). Vegetation greening has been recognized as a primary index of the recovery of karst rocky desertification (Qi et al., 2013; Yan et al., 2019). The decrease in the area of karst rocky desertification from 2005 to 2016, especially during the period 2011–2016 (Fig. 10b), was accompanied by a large increase in the NDVI from 2011 to 2016 (Fig. 4). These results are a strong indication that karst ecological restoration engineering contributed to the vegetation greening in southwest China during the last decade.

The effectiveness of karst ecological restoration engineering in regions underlain by pure carbonate rocks (limestone and dolomite) showed differences with that in other karst regions. The increase in the proportion of significant vegetation greening was greatest in the limestone region, while the smallest increase in the proportion of significant greening was coupled with the largest increased proportion of significant vegetation browning in the dolomite region (Table 2). The difference in the dissolution processes of limestone and dolomite may result in these deviations. Differential dissolution characteristics of limestone lead to the formation of underground fissures and conduits (Wang et al., 2004b). Deep underlying bedrock chemistry can have substantial effects on vegetation growth (Hahm et al., 2014), and the subsoil nutrient and organic matter supplies are substantial (Richter and Billings, 2015). Although underground leakage of surface soil and a low soil formation rate in limestone result in severe karst rocky desertification in the region where limestone dominates, the lost surface soil will gather in the fractures of the rocks to provide important root habitats for vegetation growth (Yan et al., 2019), and vegetation takes up deep water through karst conduits to resist drought stress in limestone region (Peng et al., 2019a, 2019b). Dolomite undergoes obvious overall dissolution, which occurs mainly on the surface and near-surface. Dolomite region is characterized by uniform and thin soil profiles and a high percolation rate. Compared with the limestone area, fewer underground interstices and conduits are observed in the dolomite region; consequently, a weak connection between vegetation and deep water and nutrients exist (Wang et al., 2004b). Therefore, afforestation is highly effective in the limestone area.

4.4. Implications

The large increase in the area of with an increasing NDVI in the karst regions during the conservation period indicates that karst rocky desertification is being ameliorated and the recovery of decertified karst areas is possible in southwest China. However, drought had the serious negative effects affecting vegetation growth. Our study indicated vegetation growth was generally more sensitive to drought in the karst regions than in the nonkarst region. Additionally, emerging studies have shown that afforestation consumed additional soil water and led to unintended local and regional water shortages at the regional scale (Schwärzel et al., 2019; Škerlep et al., 2020). Therefore, long-term and sustainable karst ecological restoration are needed to reduce the karst ecosystem sensitivity to climate perturbations.

The limestone region had successful afforestation, implying that limestone area can be preferred area for vegetation restoration in future afforestation projects. In addition, our study suggested the characteristics of limestone and dolomite led to different vegetation growth environment. Therefore, the effective projects of karst ecological restoration should be combined with the karst geological characteristics, such as planting trees with deep roots on the developed fissure structures of limestone region, planting herbaceous plants on dolomite area.

Karst regions occupy 13.2% of the total global land area and supply 20–25% of the drinking water worldwide (Ford and Williams, 2007; Parise et al., 2015). Karst rocky desertification, a global ecological problem, has occurred not only in southwest China but also in Europe, the Balkan Peninsula, Malaysia, Vietnam, Japan and Mexico and is expanding in Caribbean island countries, where demands on land resources are high (Jiang et al., 2014). Ecological environmental impacts, such as the loss of cultivated soil, droughts, floods and degradation of ecosystems, result from karst rocky desertification, which further worsen living conditions and aggravates poverty. The successful practices of combatting karst rocky desertification in southwest China can be applied to areas where restoration is needed and comprehensive and sustainable development can be implemented.

5. Conclusions

We investigated the spatial–temporal patterns of vegetation greening and its drivers in southwest China. The results showed that the NDVI increased significantly at a rate of 0.0026 $year^{-1}$ from 2000 to 2016, indicating a general greening trend in vegetation, and had abruptly

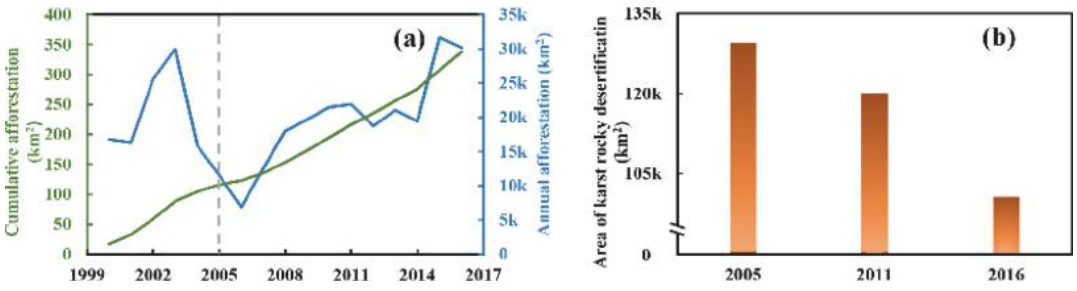

Fig. 10. Annual and cumulative afforestation area (a) and karst rocky desertification area (b) in southwest China.

increased in 2006. The area of significant vegetation greening was dramatically larger from 2006 to 2016 than from 2006 to 2016. Vegetation increased more in the karst regions, especially in limestone areas, than in the nonkarst region. Warming and precipitation promote vegetation growth under a moderate climate (2000–2005). In contrast, warming had negative effects on vegetation greening, and the positive effects between precipitation and vegetation greening, especially in the karst regions, were pronounced during dry periods (2006–2016). However, climate change generally had little direct impact on vegetation greening. The notable increases in significant vegetation greening were largely attributed to afforestation and the Grain for Green projects implemented through karst ecological engineering in 2005, which increased the forestland area by 72,571 km^2 and decreased the cropland area by 10,485 km^2 in southwest China. The karst ecological restoration measures in southwest China could serve as a reference for controlling karst rocky desertification in areas with similar environmental conditions.

CRediT authorship contribution statement

Yina Qiao: Conceptualization, Methodology, Software, Writing - original draft. **Yongjun Jiang:** Supervision, Project administration, Funding acquisition, Writing - review & editing. **Caiyun Zhang:** Visualization, Investigation, Resources.

Declaration of Competing Interest

The authors declare that they have no known competing financial interests or personal relationships that could have appeared to influence the work reported in this paper.

Acknowledgments

This study was supported by the National Key Research and Developmental Program of China (2016YFC0502306), Graduate Scientific Research and Innovation Foundation of Chongqing (CYB18073) and Chongqing Science and Technology Commission (No. cstc2018jcyjyszx0013).

References

Bai, X., Wang, S., Xiong, K., 2013. Assessing spatial-temporal evolution processes of karst rocky desertification land: indications for restoration strategies. Land Degrad. Dev. 24, 47–56.

Brandt, M., Rasmussen, K., Penuelas, J., et al., 2017. Human population growth offsets climate-driven increase in woody vegetation in sub-Saharan Africa. Nat. Ecol. Evol. 1, 0081.

Brandt, M., Yue, Y., Wigneron, J.P., et al., 2018. Satellite – observed major greening and biomass increase in south china karst during recent decade. Earth's Future 6, 1017–1028.

Cai, H., Yang, X., Wang, K., et al., 2014. Is forest restoration in the southwest China karst promoted mainly by climate change or human-induced factors? Remote Sens. 6, 9895–9910.

Cai, Z., 1989. Soil erosion in karst areas of Guangxi. J. Mountain Res. 7 (4), 255–260 (in Chinese).

Chen, C., Park, T., Wang, X., et al., 2019a. China and India lead in greening of the world through land-use management. Nat. Sustain. 2 (2), 122–129.

Chen, J., Lyu, Y., Zhao, Z., et al., 2019b. Using the multidimensional synthesis methods with non-parameter test, multiple time scales analysis to assess water quality trend and its characteristics over the past 25 years in the Fuxian Lake, China. Sci. Total Environ. 655, 242–254.

Duo, A., Zhao, W., Qu, X., et al., 2016. Spatio-temporal variation of vegetation coverage and its response to climate change in North China plain in the last 33 years. Int. J. Appl. Earth Obs. Geoinf. 53, 103–117.

Ford, D., Williams, P., 2007. Karst hydrogeology and geomorphology. Karst Hydrogeol. Geomorphol.

Gibbs, H.K., Ruesch, A.S., Achard, F., et al., 2010. Tropical forests were the primary sources of new agricultural land in the 1980s and 1990s. Proc. Nat. Acad. Sci. 107 (38), 16732–16737.

Hahm, W.J., Riebe, C.S., Lukens, C.E., et al., 2014. Bedrock composition regulates mountain ecosystems and landscape evolution. Proc. Natl. Acad. Sci. 111, 3338–3343.

Hou, W., Gao, J., Wu, S., et al., 2015. Interannual variations in growing-season NDVI and its correlation with climate variables in the Southwestern Karst Region of China. Remote Sens. 7 (9), 11105–11124.

Huber, S., Fensholt, R., Rasmussen, K., 2011. Water availability as the driver of vegetation dynamics in the African Sahel from 1982 to 2007. Global Planet Change 76, 186–195.

Hutchinson, M.F., Xu, T., 2013. ANUSPLIN Version 4.4 User Guide. The Australian National University, Canberra, Australia.

Jiang, L., Jiapaer, G., Bao, A., et al., 2017. Vegetation dynamics and responses to climate change and human activities in Central Asia. Sci. Total Environ. 599–600, 967–980.

Jiang, Z., Lian, Y., Qin, X., 2014. Rocky desertification in Southwest China: impacts, causes, and restoration. Earth Sci. Rev. 132, 1–12.

Keenan, T.F., Riley, W.J., 2018. Greening of the land surface in the world's cold regions consistent with recent warming. Nat. Clim. Change 8, 825.

King, D.A., Bachelet, D.M., Symstad, A.J., et al., 2015. Estimation of potential evapotranspiration from extraterrestrial radiation, air temperature and humidity to assess future climate change effects on the vegetation of the Northern Great Plains, USA. Ecol. Model. 297, 86–97.

Lamchin, M., Li, W.K., Jeon, S.W., et al., 2018. Long-term trend and correlation between vegetation greenness and climate variables in Asia based on satellite data. Sci. Total Environ. 618, 1089–1095.

Li, Y., Xu, H., Liu, D., 2011. Feature of the extremely severe drought in the east of Southwest China and anomalies of atmospheric circulation in summer 2006. Acta Meteorol. Sin. 25, 176–187.

Lian, Y.Q., You, G.J.Y., Lin, K.R., et al., 2015. Characteristics of climate change in southwest China karst region and their potential environmental impacts. Environ. Earth Sci. 74 (2), 937–944.

Los, S.O., 2013. Analysis of trends in fused AVHRR and MODIS NDVI data for 1982–2006: indication for a CO_2 fertilization effect in global vegetation. Global Biogeochem. Cycles 27, 318–330.

Mao, J., Ribes, A., Yan, B., et al., 2016. Human-induced greening of the northern extratropical land surface. Nat. Clim. Change 6, 959–963.

Mohsin, T., Gough, W.A., 2009. Trend analysis of long-term temperature time series in the Greater Toronto Area (GTA). Theor. Appl. Climatol. 101, 311–327.

Pan, T., Zou, X., Liu, Y., et al., 2017. Contributions of climatic and non-climatic drivers to grassland variations on the Tibetan Plateau. Ecol. Eng. 108, 307–317.

Parise, M., Closson, D., Gutiérrez, F., et al., 2015. Anticipating and managing engineering problems in the complex karst environment. Environ. Earth Sci. 74, 7823–7835.

Pei, J., Wang, L.i., Niu, Z., et al., 2019. Time series of Landsat imagery shows vegetation recovery in two fragile karst watersheds in southwest China from 1988 to 2016. Remote Sens. 11, 2044.

Peng, W., Kuang, T., Tao, S., 2019a. Quantifying influences of natural factors on vegetation NDVI changes based on geographical detector in Sichuan, western China. J. Cleaner Prod. 233, 353–367.

Peng, X., Dai, Q., Ding, G., et al., 2019b. The role of soil water retention functions of near-surface fissures with different vegetation types in a rocky desertification area. Plant Soil 441, 587–599.

Piao, S., Yin, G., Tan, J., et al., 2015. Detection and attribution of vegetation greening trend in China over the last 30 years. Glob. Change Biol. 21, 1601–1609.

Potapov, P.V., Turubanova, S.A., Tyukavina, A., et al., 2015. Eastern Europe's forest cover dynamics from 1985 to 2012 quantified from the full Landsat archive. Remote Sens. Environ. 159, 28–43.

Qi, X., Jia, J., Liu, H., et al., 2019. Relative importance of climate change and human activities for vegetation changes on China's Silk Road economic belt over multiple timescales. Catena 180, 224–237.

Qi, X., Wang, K., Zhang, C., 2013. Effectiveness of ecological restoration projects in a karst region of southwest China assessed using vegetation succession mapping. Ecol. Eng. 54, 245–253.

Qiao, Y., Chen, H., Jiang, Y., 2020. Quantifying the impacts of lithology on vegetation restoration using a random forest model in a karst trough valley, China. Ecol. Eng. 156.

Richter, D.B., Billings, S.A., 2015. 'One physical system': Tansley'secosystem as Earth's critical zone. New Phytol. 206, 900–912.

Schwärzel, K., Zhang, L., Montanarella, L., et al., 2019. How afforestation affects the water cycle in drylands: a process-based comparative analysis. Glob. Change Biol. 26 (2).

Škerlep, M., Steiner, E., Axelsson, A., et al., 2020. Afforestation driving long-term surface water browning. Glob. Change Biol. 26 (3).

Song, X., Hansen, M.C., Stehman, S.V., et al., 2018. Global land change from 1982 to 2016. Nature 563, 639.

Su, W.C., 2002. Controlling model for rocky desertification of karst mountainous region and its preventing strategy in Southwest China. J. Soil Water Convers. 16 (2) (in Chinese).

Tong, X., Brandt, M., Yue, Y., et al., 2018. Increased vegetation growth and carbon stock in China karst via ecological engineering. Nat. Sustain. 1 (1), 44–50.

Tong, X., Wang, K., Brandt, M., et al., 2016. Assessing future vegetation trends and restoration prospects in the karst regions of southwest China. Remote Sens. 8, 357.

Tong, X., Wang, K., Yue, Y., et al., 2017. Quantifying the effectiveness of ecological restoration projects on long-term vegetation dynamics in the karst regions of Southwest China. Int. J. Appl. Earth Obs. Geoinf. 54, 105–113.

Wan, L., Zhou, J., Guo, H., et al., 2016. Trend of water resource amount, drought frequency, and agricultural exposure to water stresses in the karst regions of South China. Nat. Hazards 80 (1), 23–42.

Wang, J., Wang, K., Zhang, M., et al., 2015. Impacts of climate change and human activities on vegetation cover in hilly southern China. Ecol. Eng. 81, 451–461.

Wang, K., Zhang, C., Chen, H., et al., 2019. Karst landscapes of China: patterns, ecosystem processes and services. Landscape Ecol. 34, 2743–2763.
Wang, S., Li, R., Sun, C., et al., 2004a. How types of carbonate rock assemblages constrain the distribution of karst rocky desertified land in Guizhou Province, PR China: phenomena and mechanisms. Land Degrad. Dev. 15, 123–131.
Wang, S., Liu, Q., Zhang, D., 2004b. Karst rocky desertification in Southwestern China: geomorphology, landuse, impact and rehabilitation. Land Degrad. Dev. 15 (2), 115–121.
Wessels, K.J., van den Bergh, F., Scholes, R.J., 2012. Limits to detectability of land degradation by trend analysis of vegetation index data. Remote Sens. Environ. 125, 10–22.
Yan, Y., Dai, Q., Wang, X., et al., 2019. Response of shallow karst fissure soil quality to secondary succession in a degraded karst area of southwestern China. Geoderma 348, 76–85.
Yuan, D., 2014. The Research and Countermeasures of Major Environmental Geological Problems in Karst Areas of Southwest China. Science Press, Beijing, China.
Yuan, D., Cai, G., 1987. Karst Environment. Chongqing Publish House (in Chinese).
Yuan, X., Tang, B., Wei, Y., et al., 2015. China's regional drought risk under climate change: a two-stage process assessment approach. Nat. Hazards 76, 667–684.
Zhang, M., Wang, K., Liu, H., et al., 2018. Effect of ecological engineering projects on ecosystem services in a karst region: a case study of northwest Guangxi, China. J. Cleaner Prod. 183, 831–842.
Zhou, Q., Luo, Y., Zhou, X., et al., 2018. Response of vegetation to water balance conditions at different time scales across the karst area of southwestern China-A remote sensing approach. Sci. Total Environ. 645, 460–470.
Zhu, Z., Piao, S., Myneni, R.B., et al., 2016. Greening of the Earth and its drivers. Nat. Clim. Change 6 (8), 182.